



Cite this: *Chem. Sci.*, 2021, **12**, 4503

All publication charges for this article have been paid for by the Royal Society of Chemistry

Received 1st December 2020

Accepted 3rd February 2021

DOI: 10.1039/d0sc06574a

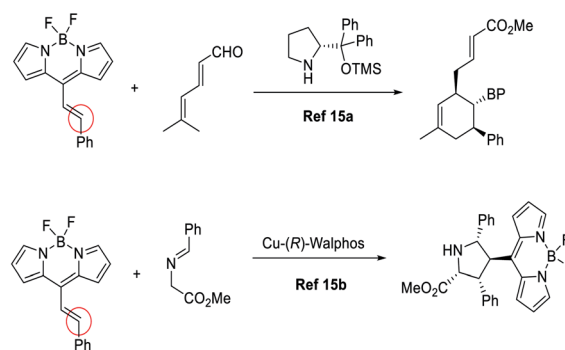
rsc.li/chemical-science

Introduction

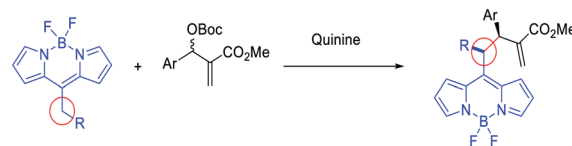
Fluorescence spectroscopy and imaging have become powerful tools in life sciences, medicine and biotechnology for their use in non-invasive analysis of living systems.¹ One of the advantages of fluorescence is its ultrasensitivity and the possibility to use it at the single molecular level.² For these reasons, boron-dipyrromethane (4,4-difluoro-4-bora-3a,4a-diaza-s-indacene, BODIPY) has been the focus of considerable interest.³ The structural versatility and spectroscopic properties such as high quantum yields and strong and tunable absorption and emission bands,⁴ besides its photostability and solubility in organic solvents, make BODIPY derivatives important tools in a wide range of fields such as biological imaging and labelling,⁵ photodynamic therapy agents,⁶ chemosensors^{3,7} and optoelectronic devices.⁸ These properties made BODIPY an important target for synthetic organic chemists. One of the main reasons for the importance of these dyes is the synthetic accessibility of BODIPYs. More precisely, functionalized BODIPYs can be easily accessible by the use of suitable functionalized pyrroles (pre-

functionalization) or by using the inherent reactivity of the BODIPY moieties (post-functionalization).⁹ This late functionalization is highly attractive due to the inherent instability of pyrroles. In recent years, several methodologies have been developed for the post-functionalization of BODIPYs, with Pd coupling being one of the most successful procedures.¹⁰

Aleman's Reaction of α,β -unsaturated BODIPY



Our approach Use of BODIPY as nucleophile in enantioselective additions:



^aFaculty of Engineering & Physical Sciences, University of Southampton, Highfield Campus, Southampton, SO17 1BJ, UK. E-mail: R.Rios-Torres@southampton.ac.uk

^bDepartamento de Química Orgánica, Facultad de Ciencias, Unidad de Excelencia de Química Aplicada a la Biomedicina y Medioambiente (UEQ), Universidad de Granada, Campus Fuentenueva, 18071, Granada, Spain

^cDepartamento de Fisicoquímica, Facultad de Farmacia, Unidad de Excelencia de Química Aplicada a la Biomedicina y Medioambiente (UEQ), Universidad de Granada, Campus Cartuja, 18071, Granada, Spain. E-mail: luiscrovetto@ugr.es

† Electronic supplementary information (ESI) available. CCDC 2013193. For ESI and crystallographic data in CIF or other electronic format see DOI: 10.1039/d0sc06574a



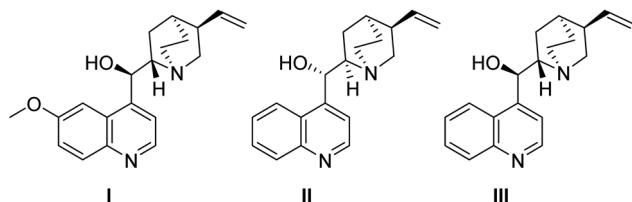
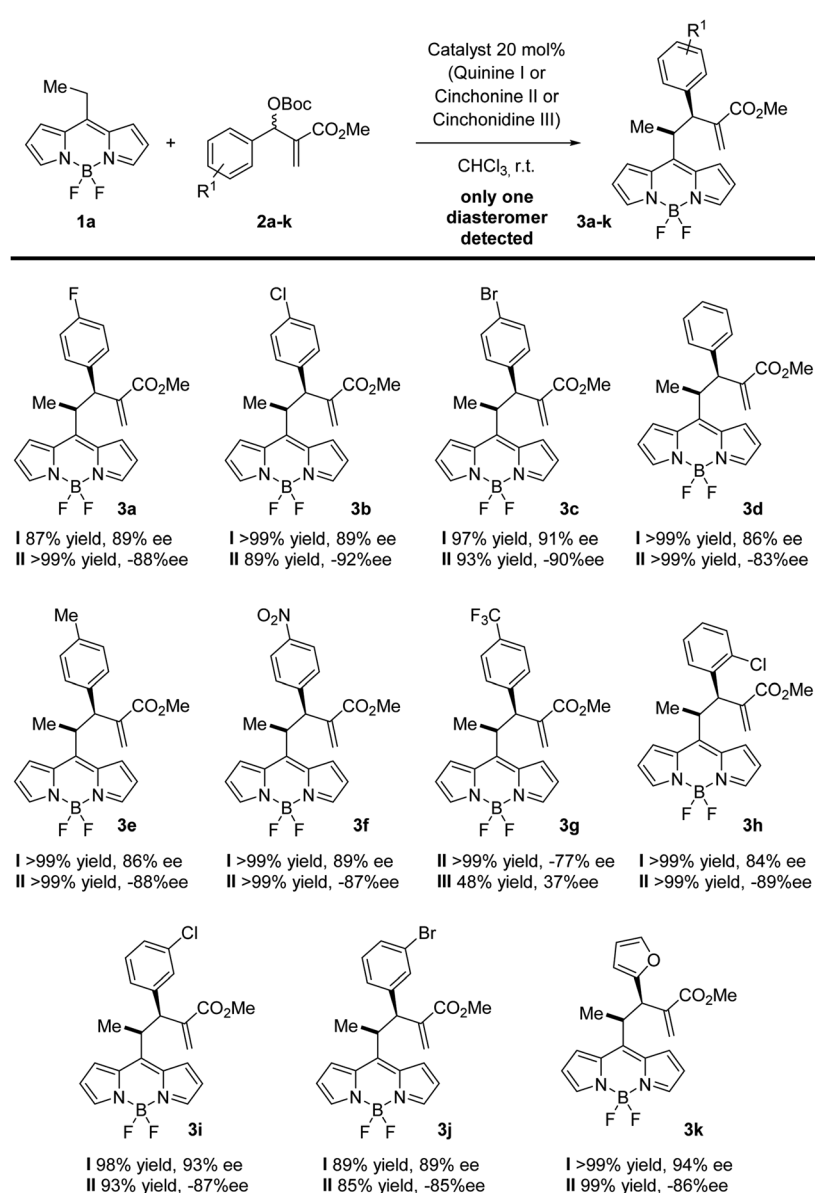


Fig. 2 Cinchona alkaloids that gave the best yields and selectivities.

Chiral BODIPYs are an attractive target, and consequently, several approaches to their synthesis have been reported.¹¹ The reason is the increasing interest in their use in chiroptical-based analytic techniques such as ECD or circularly polarized

luminescence (CPL)¹² and their use in asymmetric synthesis or as chiral probes.¹³ The introduction of chiroptical response in BODIPY-based probes is of special interest since it creates a new “spectroscopic channel”, which may minimize the background signal, a highly regarded feature in the study of complex mixtures, such as living systems. However, despite these strong interests, very few procedures have been reported, so far, for their enantioselective synthesis. The major part of the approaches is based on the introduction of chiral auxiliaries such as BINOL derivatives in place of the fluorine atoms^{12a,b,14} or on the synthesis of racemic BODIPYs that could be resolved by preparative HPLC or co-crystallization.



Scheme 1 Scope of the reaction of BODIPY **1a** with MBH **2a–k**. In a closed vial were added the organic catalyst quinine, cinchonine or cinchonidine (10 mol%), the BODIPY (0.05 mmol, 1 equiv.), the Morita–Baylis–Hillman carbonate (2 equiv.), and chloroform (1 ml) and stirred at rt for 2–10 days, monitored by ¹H-NMR. The crude was purified by flash column chromatography (*n*-hexane/EtOAc) to obtain the desired product. The regioselectivity and diastereoselectivity were determined by ¹H-NMR analysis of the crude reaction mixture (in all the examples, only one diastereomer was detected). The ee was determined by chiral HPLC.



Just at the start of the present work, Aleman and co-workers reported different enantioselective BODIPY postfunctionalization methodologies for the synthesis of enantioenriched BODIPYs,¹⁵ using BODIPYs as a suitable electron-withdrawing group for the activation of conjugated double bonds. In this way, they achieved complex bicyclic structures through trienamine catalysis^{15a} and through metal catalysed [3 + 2] cycloadditions,^{15b} with excellent results (Fig. 1).

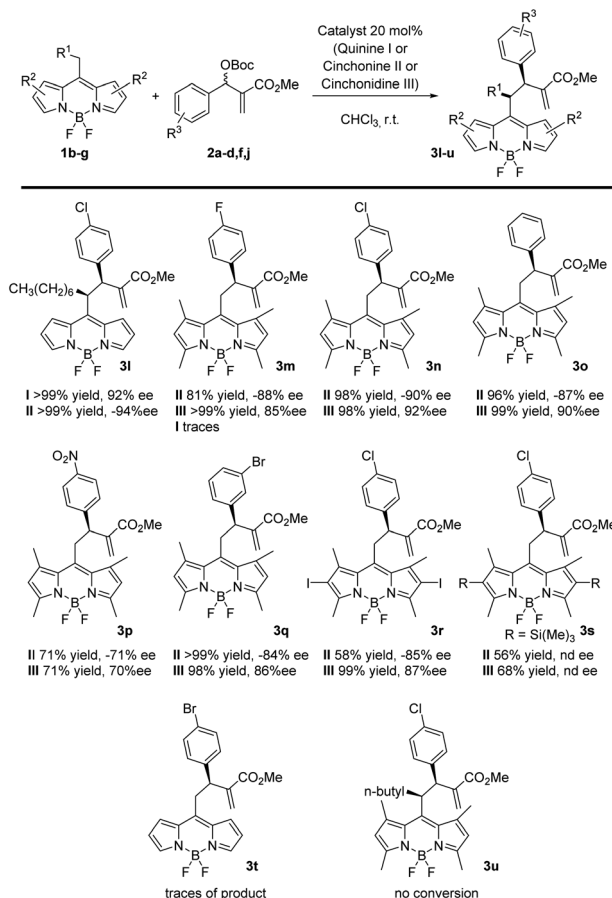
In our research group, we have developed a huge interest in the discovery and implementation of enantioselective methodologies ranging from organocatalysis to organometallic catalysis.¹⁶ With this background, we decided to study the chemistry of BODIPYs with the aim to develop easy procedures for their functionalization in an enantioselective manner, also adding several reactive handles for their easy further functional modifications.

Results and discussion

BODIPY is an excellent fluorophore as well as a strong electron withdrawing group, as shown in the studies of Alemán and others.^{15,17} Based on this observation, we envisioned that an alkylidic C–H bond linked to position 8 could be easily deprotonated and may react efficiently with suitable electrophiles. This approach would be the first example of the use of nucleophilic BODIPYs in enantioselective reactions. In order to demonstrate the soundness of our hypothesis, we selected MBH carbonates as suitable electrophiles. These substrates are well known by our group¹⁸ and can be easily activated by the presence of Lewis bases,^{18c} such as cinchona alkaloids (Fig. 2).¹⁹

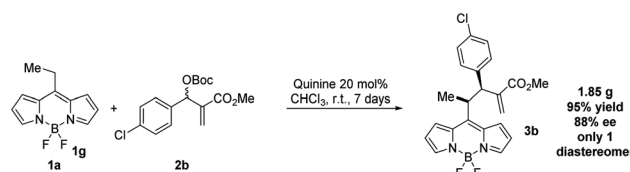
Next, we explored the scope of the reaction. In all the cases, we observed a fully diastereoselective reaction. Consequently, only one diastereomer was detected in the ¹H-NMR of the crude mixture after full conversion. Several MBH carbonates were studied in combination with the ethyl substituted BODIPY **1a**, as illustrated in Scheme 1. The catalysts used to obtain the two enantiomers of the products are quinine and cinchonine. The reaction gives the final products in excellent yields and enantioselectivities when the MBH is substituted in the *para* position with a halogen (**3a–c**), electron withdrawing group (**3f**) and electron donating group (**3e**) as well as when substituted in *meta* (**3i**, **3j**) and *ortho* (**3h**) positions. When a CF₃ substituent was present in the *para* position of the MBH (**3g**), the reaction gave lower results with catalyst **I**, and while employing **II** and **III**, a decrease in enantioselectivities was recorded, in comparison with the other substituents. High yields and enantioselectivities were also obtained when the MBH was substituted with a heterocycle (**3k**).

Next, we proceeded to study the scope of the reaction with different BODIPY derivatives, as shown in Scheme 2. When a longer alkyl chain was present in the BODIPY, the product **3l** was obtained with a complete control of the enantioselectivity and >90% yields, employing the same catalysts as in Scheme 1 (**I** and **II**). However, when a shorter chain (Me) was used, the reaction gave only traces of products (**3t**) probably due to a lower stabilization of the negative charge during the reaction. Then we expanded the reaction with a BODIPY bearing four methyl



Scheme 2 Scope of the reaction of BODIPY **1b–g** with MBH **2a–d, f, j**. In a closed vial were added the organic catalyst quinine, cinchonine or cinchonidine (20 mol%), the BODIPY (0.05 mmol, 1 equiv.), the Morita–Baylis–Hillman carbonate (2 equiv.), and chloroform (1 ml) and stirred at rt for 2–10 days, monitored by ¹H-NMR. The crude was purified by flash column chromatography (*n*-hexane/EtOAc) to obtain the desired product. The regioselectivity and diastereoselectivity were determined by ¹H-NMR analysis of the crude reaction mixture (in all the examples, only one diastereomer was detected). The ee was determined by chiral HPLC.

substituents on the pyrrole rings with differently substituted MBH. In this case, the quinine catalyst **I** gave a low conversion and was substituted with cinchonidine **III**. The reaction with MBH bearing a halogen in the *para* position (**3m**, **n**) or in the *meta* position (**3q**) and with an unsubstituted phenyl (**3o**) gave the products in high yields and enantioselectivities. Instead, lower yields were obtained with an electron withdrawing group in the *para* position (**3p**). Moderate to high yields and high



Scheme 3 Scaled up reaction with **1a**.



enantioselectivities were obtained with a BODIPY with four methyl substituents and two iodo substituents in the pyrrole rings (**3r**). When the iodo group was substituted with a trimethyl silyl group, the yields decreased and it was not possible to separate the compounds by chiral stationary phase HPLC (**3s**). When a BODIPY substituted with four methyl groups also had a longer alkyl chain as in the case of **3u**, the reaction did not work.

In order to demonstrate the robustness of the reaction, we scale up the reaction up to 1 g of **1a**. The yield and ee obtained were similar to those previously obtained (Scheme 3).

The photophysical properties were studied for all the obtained compounds; all BODIPYs were found to be fluorescent with high quantum yields and long lifetimes based on their structure (Table 1). Their absorption and fluorescence spectra were measured in a chloroform solution at 1×10^{-6} M concentration. In all cases, the absorption spectrum showed the common vibronic profile arising from the BODIPY core, with a main absorption band centered between 504 and 511 nm and a shoulder ranging from 475 to 490 nm (ESI, Fig. S1†) and a typical high extinction coefficient, which may make the compound useful for single-molecule experiments (see the ESI†). Remarkably, the absorption maximum is red shifted on those derivatives with substitution at the BODIPY core, showing the relationship between the substitution at the BODIPY core and the photophysical properties. The fluorescence spectrum after excitation at the absorption maximum was recorded from 490 to 650 nm, finding the same red shift effect as in the absorbance spectrum (ESI, Fig. S2†). Moreover, extraordinary quantum yields (Φ_F), for compound **1a**,^{20a} were found for those derivatives bearing unsubstituted BODIPY cores (**3a–l**). In contrast, lower values were found for substituted BODIPY derivatives (with the exception of compound **3o**), dropping down to 0.2 in the case of the *p*-nitro derivative **3p**. The effect of

Table 1 Photophysical parameters, absorption and fluorescence maxima, quantum yield and lifetime of the prepared compounds

Compound	Catalyst	$\lambda_{\text{abs}}^{\text{max}}$	$\lambda_{\text{flu}}^{\text{max}}$	Φ_F	τ_1/ns
3a	—	505	514	0.99	6.8357
3a	II	505	515	0.99	6.9228
3a	I	505	515	0.99	6.8745
3b	II	505	516	0.98	7.0214
3c	II	505	516	0.99	7.0289
3d	II	504	515	0.99	7.0428
3e	II	504	514	0.99	6.9434
3f	II	506	518	0.99	7.1126
3g	II	505	515	0.98	7.0343
3h	II	505	515	0.99	7.1038
3i	II	505	515	0.99	7.0463
3j	II	505	515	0.99	6.9699
3k	II	504	515	0.99	6.8506
3l	II	505	518	0.99	7.1491
3m	II	509	524	0.92	5.7655
3n	II	509	524	0.70	5.8546
3o	II	509	529	0.99	5.7833
3p	II	511	527	0.20	3.8998 ^a
3q	II	510	525	0.84	5.6729

^a A second lifetime was observed and evaluated as 0.85071 ns.

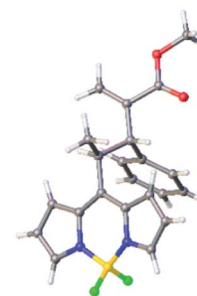


Fig. 3 X-ray crystal analysis of compound **3d**.

substitution at the BODIPY core can be also observed on the obtained fluorescence lifetimes (τ), ranging from 6.8 to 7.1 ns, in the range of compounds very similar to **1a**,^{20b,c} on compounds **3a–l** and being lower on **3m–q**.

Fortunately, the relative configuration of our compounds could be unambiguously determined by X-ray analysis of a single crystal of the racemic compound **3d** (Fig. 3), with it being *3R*,4R*/3S*,4S**.²¹ Moreover, the absolute configuration was determined by comparison of experimental and TD-DFT simulated ECD spectra.

The prototypical compound **3a** was selected for the evaluation of the chiroptical properties and for the theoretical calculations. The experimental ECD spectra of both enantiomers of **3a** were recorded in a chloroform solution (1×10^{-6} M) from 250 to 575 nm and are depicted in Fig. 4 (grey and pale red lines). The ECD spectra showed a clear signal centred at 505 nm with a dissymmetry factor ($|g_{\text{abs}}|$) value of 1×10^{-4} (ESI, Fig. S4†), in the range of the previously reported values for chiral

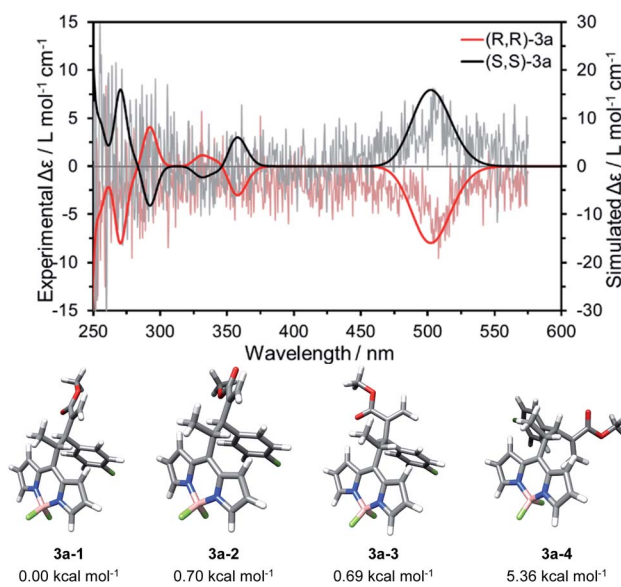


Fig. 4 Top: experimental ECD spectra of compounds (S,S)- (grey) and (R,R)-3a (pale red) measured at 1×10^{-6} M in CHCl_3 and simulated Boltzmann weighted (CAM-B3LYP/6-31G(d,p)) ECD spectra of compounds (S,S)- (black) and (R,R)-3a (red). Bottom: DFT optimized structures of the four less energetic conformers of compound (R,R)-3a and their relative Gibbs free energies (ΔG) calculated at the CAM-B3LYP/6-31G(d,p) level of theory.



BODIPYs.¹² To correlate the ECD spectra and the absolute configuration of compound **3a**, seven conformations of (*R,R*)-**3a** were optimized by DFT calculations at the CAM-B3LYP/6-31G(d,p) level of theory, and solvent effects were considered by means of the polarizable continuum model (PCM) in chloroform (ESI, Fig. S3†). In good agreement with the X-ray structure obtained for **3d**, the geometry of **3a-1** was found to be the less energetic conformation (Fig. 4). Remarkably, only four optimized conformers were found to exist at 298.15 K, according to their relative energies (Fig. 4). Subsequently, their UV-vis spectra were simulated by TD-DFT, thus obtaining the Boltzmann weighted UV-vis and ECD spectra (Fig. 4, red and black lines) at the same level of theory. The weighted ECD spectra showed an intense band ranging 475 to 550 nm, a signal at 350 nm and alternating bands at higher energy wavelengths. Thus, after comparison between the experimental and simulated spectra, we assigned the spectrum showing positive and negative Cotton effects at 505 nm to the (*S,S*) and (*R,R*) enantiomers, respectively. Therefore, we can conclude that catalyst **I** and **III** afford (*S,S*) enantiomers and **II** leads to (*R,R*) enantiomers.

In summary, we reported the first enantioselective addition of nucleophilic BODIPYs to MBH carbonates. We hope that this new approach will open a new gate for the synthesis of chiral BODIPYs using the inherent nucleophilicity of these compounds. The reaction is proficiently catalyzed by cinchona alkaloids following an $S_{N}2'-S_{N}2'$ mechanism, achieving the final compounds in excellent yields and enantioselectivities. Moreover, we are able to obtain both sets of enantiomers with similar results. The products obtained have been studied for their fluorescence emission and for their fluorescence spectroscopic properties, like absorption, fluorescence steady-state emission and fluorescence lifetime. Quantum yield has also been calculated. They typically give a high absorption coefficient and quantum yield from BODIPYs. Their long lifetime makes these compounds promising dyes to use in bioimaging studies with cells using *e.g.* a time-gated fluorescence lifetime microscopy analysis that avoids cell autofluorescence.

Experimental section

In a closed vial were added the organic catalyst quinine, cinchonine or cinchonidine (20 mol%), the BODIPY (0.05 mmol, 1 equiv.), the Morita–Baylis–Hillman carbonate (2 equiv.), and chloroform (1 ml) and stirred at rt for 2–10 days, monitored by $^1\text{H-NMR}$. The crude was purified by flash column chromatography (*n*-hexane/EtOAc) to obtain the desired product.

Conflicts of interest

There are no conflicts to declare.

Notes and references

1 (a) M. Sauer, J. Hofkens and J. Enderl, *Handbook of Fluorescence Spectroscopy and Imaging: From Single*

Molecules to Ensembles, Wiley-VCH, Weinheim, 2011; (b) M. Levitus, *Angew. Chem., Int. Ed.*, 2011, **50**, 9017.

2 (a) M. Ruedas-Rama, J. Alvarez-Pez, L. Crovetto, J. M. Paredes and A. Orte. FLIM Strategies for Intracellular Sensing, *Advanced Photon Counting*, Springer, 2014, p. 191; (b) G. De Cremer, M. B. J. Roeflaers, E. Bartholomeeusen, K. Lin, P. Dedecker, P. P. Pescarmona, P. A. Jacobs, D. E. De Vos, J. Hofkens and B. F. Sels, *Angew. Chem., Int. Ed.*, 2010, **49**, 908; (c) J. N. Mabry, M. J. Skaug and D. K. Schwartz, *Anal. Chem.*, 2014, **86**, 9451; (d) J. D. Ng, S. P. Upadhyay, A. N. Marquard, K. M. Lupo, D. A. Hinton, N. A. Padilla, D. M. Bates and R. H. Goldsmith, *J. Am. Chem. Soc.*, 2016, **138**, 3876; (e) A. Garcia IV, S. J. Saluga, D. J. Dibble, P. A. López, N. Saito and S. A. Blum, *Angew. Chem., Int. Ed.*, 2020, **59**, 1.

3 (a) A. Loudet and K. Burgess, *Chem. Rev.*, 2007, **107**, 4891; (b) N. Boens, V. Leen and W. Dehaen, *Chem. Soc. Rev.*, 2012, **41**, 1130; (c) J. Wang, N. Boens, L. Jiao and E. Hao, *Org. Biomol. Chem.*, 2020, **18**, 4135.

4 (a) J. Tao, D. Sun, L. Sun, Z. Li, B. Fu, J. Liu, L. Zhang, S. Wang, Y. Fang and H. Xu, *Dyes Pigm.*, 2019, **168**, 166; (b) S. Radunz, W. Kraus, F. A. Bischoff, F. Emmerling, H. R. Tschiche and U. Resch-Genger, *J. Phys. Chem. A*, 2020, **124**, 1787.

5 (a) Y. Ni and J. Wu, *Org. Biomol. Chem.*, 2014, **12**, 3774; (b) T. Kowada, H. Maeda and K. Kikuchi, *Chem. Soc. Rev.*, 2015, **44**, 4953; (c) R. Lincoln, L. E. Greene, W. Zhang, S. Louisiana and G. Cosa, *J. Am. Chem. Soc.*, 2017, **139**, 16273; (d) S. Kolemen and E. U. Akkaya, *Coord. Chem. Rev.*, 2018, **354**, 121; (e) S. Krajcovicova, J. Stankova, P. Dzubak, M. Hajduch, M. Soural and M. Urban, *Chem.-Eur. J.*, 2018, **24**, 4957; (f) C. S. Wijesooriya, J. A. Peterson, P. Shrestha, E. J. Gehrmann, A. H. Winter and E. A. Smith, *Angew. Chem., Int. Ed.*, 2018, **57**, 12685; (g) J. L. Donnelly, D. Offenbartl-Stiegert, J. M. Marín-Beloqui, L. Rizzello, G. Battaglia, T. M. Clarke, S. Howorka and J. D. Wilden, *Chem.-Eur. J.*, 2020, **26**, 863.

6 (a) S. G. Awuah and Y. You, *RSC Adv.*, 2012, **2**, 11169; (b) A. Kamkaew, S. H. Lim, H. B. Lee, L. V. Kiew, L. Y. Chung and K. Burgess, *Chem. Soc. Rev.*, 2013, **42**, 77; (c) Q. Zhang, Y. Cai, Q.-Y. Li, L.-N. Hao, Z. Ma, X.-J. Wang and J. Yin, *Chem.-Eur. J.*, 2017, **23**, 14307; (d) X. Guo, X. Li, X.-C. Liu, P. Li, Z. Yao, J. Li, W. Zhang, J.-P. Zhang, D. Xue and R. Cao, *Chem. Commun.*, 2018, **54**, 845; (e) E. Y. Zhou, H. J. Knox, C. J. Reinhardt, G. Partipilo, M. J. Nilges and J. Chan, *J. Am. Chem. Soc.*, 2018, **140**, 11686; (f) W. Zhang, A. Ahmed, H. Cong, S. Wang, Y. Shen and B. Yu, *Dyes Pigm.*, 2021, **185**, 108937.

7 (a) N. Kaur, P. Kaur, G. Bhatia, K. Singh and J. Singh, *RSC Adv.*, 2016, **6**, 82810; (b) Y. S. Marfin, M. V. Shipalova, V. O. Kurzin, K. V. Ksenofontova, A. V. Solomonov and E. V. Rumyantsev, *J. Fluoresc.*, 2016, **26**, 2105; (c) C. J. Reinhardt, E. Y. Zhou, M. D. Jorgensen, G. Partipilo and J. Chan, *J. Am. Chem. Soc.*, 2018, **140**, 1011.

8 (a) P.-A. Bouit, K. Kamada, P. Feneyrou, G. Berginc, L. Toupet, O. Maury and C. Andraud, *Adv. Mater.*, 2009, **21**,



1151–1154; (b) A. Bessette and G. S. Hanan, *Chem. Soc. Rev.*, 2014, **43**, 3342.

9 For interesting reviews regarding the synthesis of BODIPY derivatives, see: (a) G. Ulrich, R. Ziessel and A. Harriman, *Angew. Chem., Int. Ed.*, 2008, **47**, 1184; (b) N. Boens, B. Verbelen and W. Dehaen, *Eur. J. Org. Chem.*, 2015, 6577.

10 (a) I. J. Arroyo, R. Hub, B. Zhong Tang, F. I. López and E. Peña-Cabrera, *Tetrahedron*, 2011, **67**, 7244; (b) S. Rihn, M. Erdem, A. De Nicola, P. Retailleau and R. Ziessel, *Org. Lett.*, 2011, **13**, 1916; (c) V. Leen, P. Yuan, L. Wang, N. Boens and W. Dehaen, *Org. Lett.*, 2012, **14**, 6150; (d) G. Duran-Sampedro, E. Palao, A. R. Agarrabeitia, S. de la Moya, N. Boens and M. J. Ortiz, *RSC Adv.*, 2014, **4**, 19210; (e) Z. Feng, L. Jiao, Y. Feng, C. Yu, N. Chen, Y. Wei, X. Mu and E. Hao, *J. Org. Chem.*, 2016, **81**, 6281.

11 H. Lu, J. Mack, T. Nyokong, N. Kobayashi and Z. Shen, *Coord. Chem. Rev.*, 2016, **318**, 1.

12 (a) E. M. Saánchez-Carnerero, F. Moreno, B. L. Maroto, A. R. Agarrabeitia, M. J. Ortiz, B. G. Vo, G. Muller and S. de la Moya, *J. Am. Chem. Soc.*, 2014, **136**, 3346; (b) S. Zhang, Y. Wang, F. Meng, C. Dai, Y. Cheng and C. Zhu, *Chem. Commun.*, 2015, **51**, 9014; (c) Y. Gobo, M. Yamamura, T. Nakamura and T. Nabeshima, *Org. Lett.*, 2016, **18**, 2719; (d) F. Zinna, T. Bruhn, C. A. Guido, J. Ahrens, M. Bröring, L. Di Bari and G. Pescitelli, *Chem.-Eur. J.*, 2016, **22**, 16089; (e) M. Saikawa, T. Nakamura, J. Uchida, M. Yamamura and T. Nabeshima, *Chem. Commun.*, 2016, **52**, 10727; (f) C.-C. Shu, K.-J. Yuan, D. Dong, I. R. Petersen and A. D. Bandrauk, *J. Phys. Chem. Lett.*, 2017, **8**(1), 1–6; (g) R. Clarke, K. L. Ho, A. A. Alsimaree, O. J. Woodford, P. G. Waddel, J. Bogaerts, W. Herrebout, J. G. Knight, R. Pal, T. J. Penfold and M. J. Hall, *ChemPhotoChem*, 2017, **1**, 513; (h) C. Maeda, K. Nagahata, K. Takaishi and T. Ema, *Chem. Commun.*, 2019, **55**, 3136; (i) Z. Liu, Z. Jiang, C. He, Y. Chen and Z. Guo, *Dyes Pigm.*, 2020, **181**, 108593; (j) C. Maeda, K. Nagahata, T. Shirakawa and T. Ema, *Angew. Chem., Int. Ed.*, 2020, **59**, 7813; (k) C. Maeda, K. Suka, K. Nagahata, K. Takaishi and T. Ema, *Chem.-Eur. J.*, 2020, **26**, 4261.

13 For example: (a) H. Maeda, Y. Bando, K. Shimomura, I. Yamada, M. Naito, K. Nobusawa, H. Tsumatori and T. Kawai, *J. Am. Chem. Soc.*, 2011, **133**, 9266; (b) T. Kawasaki, M. Sato, S. Ishiguro, T. Saito, Y. Morishita, I. Sato, H. Nishino, Y. Inoue and K. Soai, *J. Am. Chem. Soc.*, 2005, **127**, 3274.

14 H.-T. Feng, X. Gu, J. W. Y. Lam, Y.-S. Zheng and B. Z. Tang, *J. Mater. Chem. C*, 2018, **6**, 8934.

15 (a) A. Guerrero-Corella, J. Asenjo-Pascual, T. J. Pawar, S. Diaz-Tendero, A. Martin-Somer, C. Villegas Lopez, J. L. Belmonte-Vazquez, D. E. Ramirez-Ornelas, E. Pena-Cabrera, A. Fraile, D. Cruz Cruz and J. Aleman, *Chem. Sci.*, 2019, **10**, 4346; (b) T. Rigotti, J. Asenjo-Pascual, A. Martin-Somer, P. Milan Rois, M. Cordani, S. Diaz-Tendero, A. Somoza, A. Fraile and J. Alemán, *Adv. Synth. Catal.*, 2020, **362**, 1345.

16 (a) M. Meazza, M. Kamlar, L. Jašiková, B. Formánek, A. Mazzanti, J. Roithová, J. Veselý and R. Rios, *Chem. Sci.*, 2018, **9**, 6368; (b) M. Meazza, G. Sitinova, C. Poderi, M. Mancinelli, K. Zhang, A. Mazzanti and R. Rios, *Chem.-Eur. J.*, 2018, **24**, 13306; (c) S. Putatunda, J. V. Alegre-Requena, M. Meazza, M. Franc, D. Rohal'ová, P. Vemuri, I. Císařová, R. P. Herrera, R. Rios and J. Veselý, *Chem. Sci.*, 2019, **10**, 4107; (d) S. Meninno, M. Meazza, J. W. Yang, T. Tejero, P. Merino and R. Rios, *Chem.-Eur. J.*, 2019, **25**, 7623.

17 Y. Liu, X. Lv, M. Hou, Y. Shi and W. Guo, *Anal. Chem.*, 2015, **87**, 11475.

18 (a) X. Companyó, G. Valero, V. Ceban, T. Calvet, M. Font-Bardía, A. Moyano and R. Rios, *Org. Biomol. Chem.*, 2011, **9**, 7986; (b) B. Wang, X. Companyó, J. Li, A. Moyano and R. Rios, *Tetrahedron Lett.*, 2012, **53**, 4124; (c) V. Ceban, P. Putaj, M. Meazza, M. B. Pitak, S. J. Coles, J. Vesely and R. Rios, *Chem. Commun.*, 2014, **50**, 7447.

19 For a review regarding enantioselective methodologies using MBH carbonates, see: R. Rios, *Catal.: Sci. Technol.*, 2012, **2**, 267.

20 (a) E. Palao, G. Duran-Sampedro, S. de la Moya, M. Madrid, C. García-López, A. R. Agarrabeitia, B. Verbelen, W. Dehaen, N. Boens and M. J. Ortiz, *J. Org. Chem.*, 2016, **81**, 3700; (b) L. Jiao, C. Yu, J. Wang, E. A. Briggs, N. A. Besley, D. Robinson, M. J. Ruedas-Rama, A. Orte, L. Crovetto, E. M. Talavera, J. M. Alvarez-Pez, M. Van der Auweraer and N. Boens, *RSC Adv.*, 2015, **5**, 89375–89388; (c) J. Bañuelos, I. J. Arroyo-Córdoba, I. Valois-Escamilla, A. Alvarez-Hernández, E. Peña-Cabrera, R. Hu, B. Zhong Tang, I. Esnal, V. Martínez and I. López Arbeloa, *RSC Adv.*, 2011, **1**, 677–684.

21 CCDC 2013193[†] (3d) contains the supplementary crystallographic data for this paper.

